

# Weights to Code: Extracting Interpretable Algorithms from the Discrete Transformer

Yifan Zhang<sup>1,2\*</sup>, Wei Bi<sup>3</sup>, Kechi Zhang<sup>1,2</sup>, Dongming Jin<sup>1,2</sup>, Jie Fu<sup>4,5†</sup>, Zhi Jin<sup>1,2†</sup>

<sup>1</sup>Key Laboratory of High Confidence Software Technology (PKU), MOE, China

<sup>2</sup>School of Computer Science, Peking University, China

<sup>3</sup>Kuaishou Technology, <sup>4</sup>Shanghai AI Lab, <sup>5</sup>Shanghai Innovation Institute

yifanzhang@stu.pku.edu.cn, fujie@pjlab.org.cn, zhijin@pku.edu.cn

## Abstract

Algorithm extraction aims to synthesize executable programs directly from models trained on specific algorithmic tasks, enabling *de novo* algorithm discovery without relying on human-written code. However, extending this paradigm to Transformer is hindered by superposition, where entangled features encoded in overlapping directions obstruct the extraction of symbolic expressions. In this work, we propose the Discrete Transformer, an architecture explicitly engineered to bridge the gap between continuous representations and discrete symbolic logic. By enforcing a strict functional disentanglement, which constrains Numerical Attention to information routing and Numerical MLP to element-wise arithmetic, and employing temperature-annealed sampling, our method effectively facilitates the extraction of human-readable programs. Empirically, the Discrete Transformer not only achieves performance comparable to RNN-based baselines but crucially extends interpretability to continuous variable domains. Moreover, our analysis of the annealing process shows that the efficient discrete search undergoes a clear phase transition from exploration to exploitation. We further demonstrate that our method enables fine-grained control over synthesized programs by imposing inductive biases. Collectively, these findings establish the Discrete Transformer as a robust framework for demonstration-free algorithm discovery, offering a rigorous pathway toward Transformer interpretability.

## 1 Introduction

Program synthesis is the task to construct a program that provably satisfies a given high-level formal specification, a line of work dating back to Church (1963). In recent years, this field has been revolutionized by Large Language Models (LLMs), which have achieved remarkable success

in code generation (Rozière et al., 2024; Guo et al., 2024; Team et al., 2024). Despite their success, an alternative paradigm—*algorithm extraction*—offers a distinct advantage: the ability to derive algorithms *de novo*, thereby potentially uncovering innovative solutions independent of human-generated data (Michaud et al., 2024). Recent work has demonstrated the feasibility of this direction for Recurrent Neural Networks (RNNs) via the Mechanistic-Interpretability-based Program Synthesis (MIPS), which leverages symbolic regression to synthesize programs matching network behavior (Michaud et al., 2024).

However, extending algorithm extraction to the dominant Transformer architecture faces significant challenges, rooted in a fundamental gap between the continuous, high-dimensional nature of Transformer and the discrete, sparse nature of symbolic algorithms. The primary obstacle lies in interpreting the Transformer’s internal representations. Specifically, the standard Transformer often exhibits “superposition”, where features are encoded in an overlapping, non-orthogonal set of directions rather than individual neurons (Cunningham et al., 2023; Elhage et al., 2022). Consequently, the model’s internal representations are highly entangled and polysemantic. Unlike the disentangled input-output mappings required for symbolic regression, these representations render the direct extraction of explicit symbolic expressions infeasible. This motivates our central question: *Is it possible to synthesize executable and interpretable programs by extracting algorithms from Transformer?*

In this work, we propose the *Discrete Transformer*, an architecture explicitly optimized for algorithm extraction (see Figure 1). Building upon the framework of Transformer Programs (Friedman et al., 2023), our design incorporates critical modifications to facilitate the transition from continuous dynamics to discrete logic. Architecturally, the Discrete Transformer comprises Numerical At-

\*Work done during an internship at Kuaishou Technology.

†Corresponding authors.

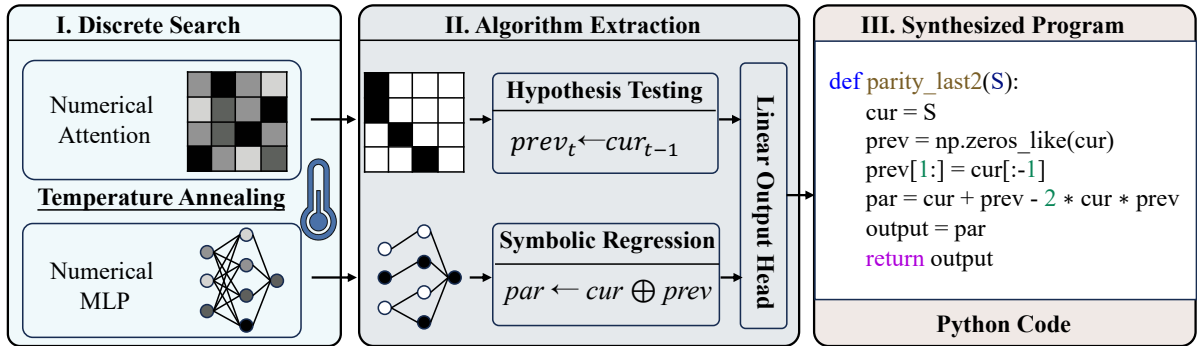


Figure 1: Illustration of the proposed framework for extracting executable algorithms from a Discrete Transformer. (I) Discrete Search: Temperature annealing is leveraged to encourage interpretable discretization in both Numerical Attention and MLP modules. (II) Algorithm Extraction: Attention patterns are characterized via hypothesis testing (e.g., identifying token shifts), while arithmetic transformations are approximated through symbolic regression. (III) Synthesized Program: The extracted components are integrated via a linear output head to generate Python code. As shown, the framework successfully recovers the `parity_last2` algorithm, correctly implementing the arithmetic XOR logic.

tention, Numerical MLP, and a linear output head. Aligning with the Restricted Access Sequence Processing (RASP) computational model (Weiss et al., 2021), we impose a strict functional disentanglement, where Numerical Attention is responsible for routing information across positions, while the Numerical MLP is dedicated solely to element-wise arithmetic operations. Crucially, we incorporate differentiable sampling mechanisms into each module to inject temperature-controlled discreteness. Through annealing, the model gradually transitions into a fully discrete representation, ensuring that the solution to the algorithmic task is implicitly but clearly encoded within its weights.

Once the model converges to a discrete state, we employ a modular strategy to recover the underlying algorithm. Recognizing the distinct roles of the components, we adopt *hypothesis testing* for the Attention modules to identify interpretable routing patterns, and apply *symbolic regression* to the MLP modules to infer the specific arithmetic expressions. Finally, these extracted primitives are aggregated through the linear output head, yielding a concise, human-readable, and executable program that verifiably solves the target task.

We validate our approach on a diverse suite of algorithmic tasks, including the MIPS benchmark (Michaud et al., 2024). Crucially, unlike prior RNN-based methods restricted to discrete data domains, our Discrete Transformer natively processes continuous variables, substantially broadening the scope of mechanistic-interpretability-based program synthesis. Beyond performance, we provide

a rigorous analysis of the framework’s theoretical and empirical properties. In addition to revealing that functional convergence precedes full structural discretization (Louizos et al., 2018; Savarese et al., 2021), we demonstrate that tailoring architectural constraints imposes strong inductive biases, establishing the Discrete Transformer as a controllable framework for interpretable algorithm discovery.

Overall, our main contributions are as follows:

- We propose the Discrete Transformer, a RASP-aligned architecture that enforces functional disentanglement to bridge continuous optimization and discrete logic.
- We develop a modular extraction pipeline combining hypothesis testing and symbolic regression, extending mechanistic-interpretability-based synthesis to continuous variables.
- We provide rigorous analysis validating the effectiveness of imposed inductive biases for controllable algorithm discovery.

## 2 Related Work

### 2.1 Mechanistic Interpretability in Transformer

Foundational to connecting Transformer with programs is the RASP (Weiss et al., 2021), which abstracts sequence processing into primitives. While Tracr (Lindner et al., 2023) compiles programs into weights, Transformer Programs (Friedman et al., 2023) address the inverse problem, utilizing Gumbel-Softmax (Jang et al., 2017) to learn discrete structures, which can be deterministically mapped to programs. However, we argue that such

direct translation merely simulates low-level operations on test cases; true algorithm extraction requires explicit symbolic reasoning to distill abstract, high-level algorithm logic.

## 2.2 Symbolic Regression and Algorithm Extraction

Symbolic regression searches for closed-form expressions balancing accuracy and complexity (Udrescu et al., 2020; Cranmer, 2023). While traditionally used for scientific discovery (Cranmer et al., 2020; Ma et al., 2022) or recently enhanced by LLMs’ scientific priors (Shojaee et al., 2025), we leverage it as an engine for algorithm extraction. Here, the objective shifts from data fitting to synthesizing concise, human-readable programs directly from trained neural networks.

The innovative MIPS framework (Michaud et al., 2024) pioneers this approach for RNNs. Analogous to the use of Sparse Autoencoders (SAEs) in interpreting features (Cunningham et al., 2023; Bricken et al., 2023), the MIPS employs integer autoencoders to approximate continuous latent states into finite states suitable for symbolic regression. In contrast to the MIPS, which relies on auxiliary quantization modules to approximate discreteness post-hoc, our Discrete Transformer is architecturally designed to learn interpretable, discrete representations directly, enabling direct and seamless algorithm extraction.

## 3 Discrete Transformer

In this section, we introduce the Discrete Transformer, a specialized architecture purposefully designed for symbolic regression and algorithm extraction. It is structured as a computational graph with clear functional specialization: Numerical Attention performs explicit variable routing, while the Numerical MLP is responsible for arithmetic computation.

### 3.1 Numerical Residual Stream

The essential difference between the Discrete Transformer and the standard one lies in the structure of the residual stream and the mechanism of information processing. To align with the symbolic nature of algorithm extraction, we define the residual stream not as latent vectors, but as a collection of explicit scalar variables. Let  $\mathbf{h}_l = [x_1, \dots, x_{N_l}]^\top \in \mathbb{R}^{N_l}$  denote the residual stream at layer  $l$ , consisting of  $N_l$  distinct scalar variables.

In contrast to standard additive updates, we adapt the concatenation principle (Friedman et al., 2023; Lai-Dang et al., 2025) to the scalar domain, updating the residual stream with new outputs  $\mathbf{o}_l$ :

$$\mathbf{h}_{l+1} = \text{Concat}(\mathbf{h}_l, \mathbf{o}_l) \in \mathbb{R}^{N_l + |\mathbf{o}_l|}. \quad (1)$$

This design preserves the full computational history as disentangled coordinates, alleviating the information interference induced by superposition in dense vectors.

Moreover, a critical challenge in algorithm extraction is to identify *which* variables serve as operands. Inspired by learnable input selection (Friedman et al., 2023), we address this by designing a discretized reading mechanism tailored for the numerical residual stream: for any computational module (Numerical Attention or MLP) at layer  $l$  requiring  $k$  inputs, we learn a projection matrix  $\mathbf{W}_{\text{read}} \in \mathbb{R}^{k \times N_l}$  to select inputs from the residual stream  $\mathbf{h}_l$ . To enable discrete structure optimization within a differentiable framework, we apply a temperature-controlled sampling function  $S(\cdot, \tau)$  (derivation provided in Appendix A) row-wise to the logits  $\mathbf{W}_{\text{read}}$ . The input vector  $\mathbf{u} \in \mathbb{R}^k$  is then retrieved from the current residual stream  $\mathbf{h}_l \in \mathbb{R}^{N_l}$  via:

$$\mathbf{u} = S(\mathbf{W}_{\text{read}}, \tau) \cdot \mathbf{h}_l, \quad (2)$$

where  $\tau$  is the annealing temperature. As temperature  $\tau \rightarrow 0$ , the selection distribution converges to a deterministic one-hot indicator, effectively functioning as a differentiable pointer over the computation graph.

### 3.2 Numerical Attention as Router

Following the architectural paradigm established in Tracr (Lindner et al., 2023) and Transformer Programs (Friedman et al., 2023), we employ a hard attention mechanism designed strictly as an information routing operator, rather than a feature mixer. In the context of algorithm extraction, this design can help isolate all computational transformations within simpler MLP, thereby reducing the difficulty of attention analysis.

**Piecewise Linear Encoding.** Since the residual stream consists of raw scalars ( $\mathbf{h}_l \in \mathbb{R}^{N_l}$ ), distinct scalar variables lack the high-dimensional expressivity required for effective dot-product comparisons. To address this, we define the query and key as selected scalars  $x_q, x_k \in \mathbb{R}$ , and project them into a higher-dimensional space using the

Piecewise Linear Encoding (PLE) (Gorishniy et al., 2022):

$$\mathbf{q} = \phi_{\text{PLE}}(x_q), \quad \mathbf{k} = \phi_{\text{PLE}}(x_k), \quad (3)$$

where  $\mathbf{q}, \mathbf{k} \in \mathbb{R}^{d_{\text{attn}}}$  and  $\phi_{\text{PLE}} : \mathbb{R} \rightarrow \mathbb{R}^{d_{\text{attn}}}$  is a learnable mapping.

**Deterministic Attention Mechanism.** The attention scores  $\mathbf{a}_{\text{raw}} \in \mathbb{R}^N$  over a context length  $N$  are computed via scaled dot-product with T5-style relative positional biases  $\mathbf{b}_{\text{rel}}$  (Raffel et al., 2023):

$$\mathbf{a}_{\text{raw}} = \frac{\mathbf{K}\mathbf{q}}{\sqrt{d_{\text{attn}}}} + \mathbf{b}_{\text{rel}}, \quad (4)$$

where  $\mathbf{K} \in \mathbb{R}^{N \times d_{\text{attn}}}$  stacks the projected keys from the context. To ensure interpretable attention patterns, we enforce hard attention using the sampling function  $S(\cdot)$ . Crucially, the value projection is the identity function for scalars, meaning that the value vector  $\mathbf{v} \in \mathbb{R}^N$  consists directly of the raw scalars from the history. The output  $o_{\text{attn}} \in \mathbb{R}$  is a weighted sum:

$$o_{\text{attn}} = S(\mathbf{a}_{\text{raw}}, \tau) \cdot \mathbf{v}. \quad (5)$$

This design forces the attention head to converge to a deterministic pointer operation, retrieving specific raw values from history (e.g., “copy the value from the token at offset -1”).

### 3.3 Numerical MLP as Operator

While the Attention handles data movement, the Numerical MLP is dedicated to element-wise arithmetic and logical transformations. Drawing on the insight that Transformer MLPs contribute additive updates to the residual stream, which can be decomposed into weighted sums of sub-updates (Geva et al., 2022), we explicitly decompose the MLP module into a collection of parallel, independent sub-modules (sub-MLPs).

Each sub-module performs a single elementary operation. It first selects a small, fixed number of scalars (typically  $k = 2$ ) from the stream via the discretized reading mechanism, forming an operand vector  $\mathbf{u} \in \mathbb{R}^k$ . These operands are processed by a shallow network:

$$o = \mathbf{W}_2(\sigma(\mathbf{W}_1\mathbf{u} + \mathbf{b}_1)) + b_2, \quad (6)$$

where  $\mathbf{W}_1 \in \mathbb{R}^{d_{\text{hid}} \times k}$ ,  $\mathbf{W}_2 \in \mathbb{R}^{1 \times d_{\text{hid}}}$  are learnable weights,  $\mathbf{b}_1, b_2$  are biases, and  $\sigma$  is a non-linear activation (e.g., ReLU). The resulting scalar output  $o$  is concatenated back to the residual stream.

**Inductive Bias for Symbolic Regression.** By severely constraining the input dimension  $k$  and the hidden width  $d_{\text{hid}}$ , we deliberately limit the complexity of each sub-module. This bottleneck forces the network to decompose complex functions into a sequence of simple arithmetic steps, creating ideal conditions for symbolic regression (e.g., PySR (Cranmer, 2023)) to extract closed-form expressions.

### 3.4 Linear Output Head

The architecture concludes with a linear output head that aggregates the discrete computational steps into a final prediction:

$$\hat{y} = \mathbf{w}_{\text{out}}^\top \mathbf{h}_{\text{final}}, \quad (7)$$

where  $\mathbf{h}_{\text{final}}$  is the final residual stream, and  $\mathbf{w}_{\text{out}}$  represents the aggregation weights. To reduce the length of the extracted program, we impose a sparsity threshold  $\epsilon$  on the magnitude of the weights (i.e., set  $w_i = 0$  if  $|w_i| < \epsilon$ ). This prunes unnecessary intermediate variables from the computation graph, retaining only the paths essential for the task. The final trained model thus represents a clean, executable computational graph: nodes correspond to either routing operations (Attention) or arithmetic functions (MLP), and edges are defined by the discrete selections of the discretized reading modules.

## 4 From Weights to Code

After training with temperature annealing, the converged Discrete Transformer reaches a fully discrete state, and the algorithmic solution is implicitly encoded within its sparse weights and activation patterns. To recover an explicit, human-readable program, we treat the trained model as a computational graph composed of two distinct types of nodes: *routers* (Attention) and *operators* (MLP). We propose a decoupled extraction pipeline that first infers the function of each node using component-specific strategies, then reconstructs the global program trace via backward traversal.

### 4.1 Hypothesis Testing for Attention

For the Numerical Attention module, extracting explicit expressions via direct symbolic regression is challenging due to the computational complexity in the PLE of queries and keys, dot-product interactions, and the hard attention mechanism induced by sampling functions. However, since the structural role of attention is constrained to be an information router, we abstract away from the intermediate

arithmetic and focus our interpretability analysis on the resulting routing patterns.

We conceptualize the Numerical Attention module as a deterministic pointer performing differentiable addressing on context memory. Following Neural Turing Machines (Graves et al., 2014), we categorize addressing into *Location-based* (position-dependent) and *Content-based* (value-dependent). We hypothesize that our attention heads specialize into these two modes, and empirically observe that they manifest as two typical interpretable patterns: *Fixed Offset* and *Windowed Extrema*.

Specifically, for a given head, we analyze its attention matrices generated over the validation set. We test the hypotheses by examining the statistical properties across the dataset:

- *Fixed Offset*. This pattern corresponds to relative positional indexing. We hypothesize that there exists an integer offset  $\delta$  such that, for a large fraction of query positions  $i$ , the head places most of its attention on  $j = i - \delta$ . We operationalize this by measuring whether the averaged attention mass concentrates on a single offset diagonal (corresponding to  $j = i - \delta$ ) beyond a predefined threshold.
- *Windowed Extrema*. This pattern reflects content-dependent selection. Let  $\mathbf{v} \in \mathbb{R}^N$  be the sequence of scalar values, where  $v_j$  is the value at position  $j$ . We hypothesize that there exists a window size  $z \in \mathbb{Z}^+$  such that, for a large fraction of query positions  $i$ , the head attends primarily to  $j^* = \arg \min / \max_{j \in \{i-z+1, \dots, i\}} v_j$ . We verify this hypothesis by checking the sample-wise agreement between the head’s selected index and the true extremum index within the window.

Across the benchmark investigated, we find these simple routing patterns achieve high coverage of active heads. The few “unmatched heads” represent computational noise—being negligible in magnitude or acting as redundant variables—and do not influence the logic of the final assembled program (see Appendix B for detailed analysis).

## 4.2 Symbolic Regression for MLP

In contrast to the Attention, the Numerical MLP modules serve as the arithmetic core. Thanks to the disentangled architecture, each MLP sub-module functions as an isolated mapping  $f : \mathbb{R}^k \rightarrow \mathbb{R}$  with low-dimensional inputs (typically  $k = 2$ ). This architectural isolation makes them ideal candidates for black-box symbolic regression.

For each sub-MLP, we collect a dataset of input-

output pairs  $\mathcal{D} = \{(\mathbf{u}^{(i)}, o^{(i)})\}_{i=1}^M$  from validation passes. We employ the PySR (Cranmer, 2023), a symbolic regression tool based on genetic algorithms, to search for the optimal symbolic expression  $\hat{f}$  that minimizes the error on  $\mathcal{D}$ . Crucially, the constrained input dimension and limited model capacity drastically reduce the search space, enabling the PySR to reliably converge to exact arithmetic expressions (e.g.,  $o = 2u_1 + u_2$ ) rather than approximate fits.

## 4.3 Global Program Assembly

The final phase integrates these extracted primitives into a coherent program. The linear output head,  $\hat{y} = \mathbf{w}_{\text{out}}^\top \mathbf{h}_{\text{final}}$ , serves as the entry point for extraction. We first apply magnitude-based pruning to  $\mathbf{w}_{\text{out}}$  ( $|w_i| > \epsilon$ ) to identify the active variables contributing to the final prediction.

Starting from these active variables, we perform a *backward traversal* of the computational graph. Recursively, we replace each intermediate variable in the residual stream with its corresponding symbolic definition, either a deterministic pointer from Attention or a distilled arithmetic expression from MLP, until the traversal reaches the raw input tokens. This process effectively compiles the neural network into concise, closed-form algorithmic expressions that approximate the Discrete Transformer’s behavior with high fidelity across the relevant input domain.

## 5 Experiments

In this section, we evaluate the Discrete Transformer on a diverse suite of algorithmic reasoning tasks. We aim to demonstrate that, beyond achieving high performance, our model extracts interpretable and human-readable algorithms, thereby revealing the underlying structure and logic inherent in the data.

**Datasets** We utilize the MIPS benchmark (Michaud et al., 2024) to probe capabilities ranging from local computation to global state tracking<sup>1</sup>. The tasks are categorized into three groups: (1) *Linear Arithmetic* (e.g., `sum_last2`, `sum_last`); (2) *Non-Linear Composition* (e.g., `parity_last2`, `add_mod_3`) which requires approximating non-linear logic; and (3) *Dynamical Systems* (e.g., `gravity`) to evaluate the discovery of physical

<sup>1</sup>State tracking refers to the maintenance and updating of an explicitly updated state across the input sequence (e.g., a cumulative sum). (Zhang et al., 2025), as opposed to purely local computations.

Table 1: Performance of the Discrete Transformer on the algorithm benchmark. For these regression tasks, loss is reported as MSE on the test set. The model demonstrates strong predictive performance across the benchmark, with loss values close to zero.

Task	Loss	Task	Loss
<i>Linear Arithmetic</i>			
sum_last2	$6.76 \times 10^{-9}$	diff_last2	$7.02 \times 10^{-16}$
sum	$1.70 \times 10^{-14}$		
<i>Non-Linear Composition</i>			
parity_last2	$1.46 \times 10^{-12}$	max_prev2	$4.43 \times 10^{-6}$
min_prev2	$1.77 \times 10^{-5}$	bitwise_and	$1.06 \times 10^{-18}$
bitwise_or	$1.63 \times 10^{-6}$	bitwise_not	$< 10^{-20}$
bitwise_xor	$6.67 \times 10^{-20}$	abs	$5.25 \times 10^{-14}$
abs_of_diff	$2.01 \times 10^{-8}$	parity	$8.09 \times 10^{-17}$
add_mod_3	$1.72 \times 10^{-7}$		
<i>Physical Problems</i>			
freebody	$9.57 \times 10^{-11}$	gravity	$1.86 \times 10^{-11}$
spring	$3.49 \times 10^{-9}$		

laws. Detailed definitions for all tasks are provided in Appendix C.

**Training Details** All models employ a decoder-only architecture implemented in PyTorch, optimized via AdamW to minimize the Mean Squared Error (MSE). We train for 50 epochs (100 for physical tasks) with a batch size of 512 and cosine learning rate decay. Crucially, to handle discrete optimization, we apply geometric annealing to the sampling temperature  $\tau$ , decreasing it from 10.0 to 0.1. We report the average performance across three random seeds, with hyperparameters (layers, heads, sub-MLPs) selected via grid search. Full hyperparameters and grid search ranges are detailed in Appendix C.

**Results** We evaluate the Discrete Transformer across the diverse task suite. As shown in Table 1, the Discrete Transformer achieves near-perfect convergence across all task categories, with test losses approaching zero. Beyond numerical accuracy, our primary contribution lies in demonstrating that the solution embedded within the Discrete Transformer can be successfully extracted into human-readable code, which matches the capabilities of MIPS on this benchmark. By applying the methodology detailed in Section 4, we successfully compile the trained weights into executable Python code. We highlight three key findings below.

- **Discovery of Algorithmic Parsimony in Linear Tasks.** In linear tasks, the discrete optimization process demonstrates a strong inductive bias towards *parsimony*. The model frequently learns to bypass the Numerical MLP entirely, leveraging the linear

output head to perform arithmetic directly. For instance, in `sum_last2` (Figure 2), the model assigns specific attention heads to retrieve  $x_{t-1}$  (via a verified “Fixed Offset” pattern) and integrates it with the current token  $x_t$ . Symbolic simplification yields the exact expression  $y_t = x_t + x_{t-1}$ ,<sup>2</sup> effectively capturing the underlying addition logic.

- **Exact Recovery of Non-Linear Identities.** For tasks requiring non-linear logic, the extraction methodology successfully identifies algebraically equivalent expressions. For instance, in the `parity_last2` task ( $x_t \oplus x_{t-1}$ ) with binary inputs  $x \in \{0, 1\}$ , simplifying the extracted expressions (Figure 3) yields  $y_t = x_t + x_{t-1} - 2x_t x_{t-1}$ , which is an exact algebraic formulation of the parity operation. For `maximum_prev2` and `minimum_prev2` tasks, simplifying the extracted expressions in Figure 4 reveals a piecewise-linear implementation of conditional computation via ReLU operations:  $\max(x_t, x_{t-1}) = x_{t-1} + \text{ReLU}(x_t - x_{t-1})$  and  $\min(x_t, x_{t-1}) = x_{t-1} - \text{ReLU}(x_{t-1} - x_t)$ . This demonstrates the capability to reverse-engineer black-box neural computations into explicit algebraic forms equivalent to logical operations.

- **Modeling Continuous Dynamics.** In physical tasks such as `gravity`, the Discrete Transformer effectively identifies the essential computational variables and successfully constructs the correct computation graph through the coordination of the Numerical Attention, Numerical MLP, and output head, demonstrating strong potential for modeling complex physical processes. Moreover, owing to its inherent model design, it offers a clear advantage over prior symbolic synthesis approaches. Specifically, the MIPS is inherently restricted to discrete data domains, rendering it inapplicable to floating-point tasks. In contrast, the Discrete Transformer natively supports continuous variables. This distinction enables the extraction of algorithms that capture continuous dynamics, substantially broadening the scope of mechanistic-interpretability-based program synthesis.

## 6 Further Analysis

In this section, we provide a rigorous analysis of the Discrete Transformer’s properties, positioning it at the intersection of program synthesis and continuous sparsification. We primarily focus on the

<sup>2</sup>We employ the SymPy library (Meurer et al., 2017) to automatically simplify the extracted expressions, leading to more concise and readable mathematical formulae.

```

1 import numpy as np
2 def sum_last2(input_seq):
3     # V0_input
4     input_arr = np.array(input_seq, dtype=float)
5     seq_len = input_arr.shape[0]
6     V0 = input_arr[:, 0]
7     # V1_Attn_L0H0
8     V1 = np.zeros(seq_len)
9     # Fixed offset 1
10    V1[1:] = V0[:-1]
11    # V2_Attn_L0H1
12    V2 = np.zeros(seq_len)
13    # Fixed offset 1
14    V2[1:] = V0[:-1]
15    # Output Head
16    output = 1.00 * V0 + 1.00 * V1 + 0.01 * V2
17    return output

```

↓ *symbolic simplification*

**Simplified Expression:**  $y_t = x_t + x_{t-1}$

Figure 2: Algorithm extraction results for the `sum_last2` task. Modules are denoted by their type and indices (e.g., `Attn_L0H0` represents the attention head at index 0 of layer 0). The extracted code reveals that the model utilizes specific attention heads to retrieve the previous token. Symbolic simplification (bottom) shows the mathematically simplified expression, verifying that the model correctly learns the logic  $y_t = x_t + x_{t-1}$ .

training dynamics, characterizing a distinct phase where functional convergence is achieved prior to complete structural discretization. We further demonstrate how architectural constraints serve as strong inductive biases, establishing the model as a controllable testbed for interpretable algorithm discovery.

### 6.1 Continuous-to-Discrete Homotopy

We frame program synthesis as a continuous-to-discrete homotopic transformation. From the perspective of differentiable architecture search and continuous sparsification (Louizos et al., 2018; Jang et al., 2017), we relax the discrete constraint by introducing continuous structural parameters, specifically the projection matrices  $\mathbf{W}_{\text{read}}$ . The temperature  $\tau$  serves as a homotopy parameter: high values define a search space over the continuous probability simplex for exploration, while annealing  $\tau \rightarrow 0$  smoothly deforms the distribution toward simplex vertices for exploitation.

To validate these dynamics, in addition to the MSE loss (serving as the soft training objective  $\mathcal{L}_{\text{soft}}$ ), we monitor two metrics: Structural Agreement ( $\mathcal{A}(e)$ ) and Discretization Dis-

```

1 import numpy as np
2 def parity_last2(input_seq):
3     # V0_input
4     input_arr = np.array(input_seq, dtype=float)
5     seq_len = input_arr.shape[0]
6     V0 = input_arr[:, 0]
7     # V1_Attn_L0H0
8     V1 = np.zeros(seq_len)
9     # Fixed offset 1
10    V1[1:] = V0[:-1]
11    # V2_Attn_L0H1
12    V2 = np.zeros(seq_len)
13    # Fixed offset 1
14    V2[1:] = V0[:-1]
15    # V3_MLP_L0M0
16    V3 = ((V1 + -0.41) * ((V0 - 0.41) * 3.57)) + -0.61
17    # Output Head
18    output = -0.56 * V3 + 0.17 * V0 + 0.10 * V2 + 0.07 *
19    V1
20    return output

```

↓ *symbolic simplification*

**Simplified Expression:**  $y_t = x_t + x_{t-1} - 2x_t x_{t-1}$

Figure 3: Algorithm extraction results for the `parity_last2` task. The extracted code reveals that the model utilizes specific attention heads (e.g., `Attn_L0H0`) to retrieve the previous token, and specific sub-MLPs (e.g., `MLP_L0M0`) to perform non-linear transformations. The bottom panel presents the symbolic simplification  $y_t = x_t + x_{t-1} - 2x_t x_{t-1}$ , which is the algebraic formulation of the parity logic.

crepancy ( $\Delta(e)$ ). Let  $\{\mathbf{p}_r^{(e)}\}_{r=1}^R$  be the set of all row-wise probability distributions derived from  $S(\mathbf{W}_{\text{read}}, \tau)$  at epoch  $e$ ,  $E$  the total number of epochs, and  $\mathcal{L}_{\text{hard}}(e)$  the hard loss computed via deterministic argmax sampling. We define  $\mathcal{A}(e) = \frac{1}{R} \sum_{r=1}^R \mathbb{I}(\arg \max \mathbf{p}_r^{(e)} = \arg \max \mathbf{p}_r^{(E)})$ . And we further define  $\Delta(e) = \mathcal{L}_{\text{hard}}(e) - \mathcal{L}_{\text{soft}}(e)$ . As shown in Figure 5, we observe a distinct phase transition: the significant decline in  $\Delta(e)$  occurs slightly later than that of  $\mathcal{L}_{\text{soft}}$ , concurrently with  $\mathcal{A}(e)$  approaching 1.0 as annealing proceeds. This lag suggests a two-stage process where the model first achieves *soft convergence*—learning functional mappings via relaxed representations—before undergoing *structural crystallization*, thereby ensuring a robust transition from exploration to exploitation.

### 6.2 Controllability via Inductive Biases

Unlike standard code LLMs, which synthesize programs based on opaque statistical patterns, our Discrete Transformer offers a unique advantage:

```

1 import numpy as np
2 def relu(x):
3     return np.maximum(0, x)
4 def extrema_prev2(input_seq, mode):
5     # V0_input
6     input_arr = np.array(input_seq, dtype=float)
7     seq_len = input_arr.shape[0]
8     V0 = input_arr[:, 0]
9     # V1_Attn_L0H0
10    V1 = np.zeros(seq_len)
11    # Fixed offset 1
12    V1[1:] = V0[:-1]
13    # V3_MLP_L0M0, Output Head
14    if mode == 'max': # maximum_prev2
15        V3 = (((V0 * -0.12) + relu((V1 * -1.00) + V0)) *
16            -2.21) + ((V1 * -0.26) / 1.02)
17        output = 0.88 * V1 + -0.45 * V3 + 0.12 * V0
18    else: # minimum_prev2
19        V3 = 1.43 * (V0 + (((3.49 * relu(V1 - V0)) - V1) -
20        (V1 * 1.04)))
21        output = 0.42 * V1 + 0.29 * V0 + -0.20 * V3
22    return output

```

↓ symbolic simplification

**Simplified Expression:**  $\max(x_t, x_{t-1}) = x_{t-1} + \text{ReLU}(x_t - x_{t-1})$ ,  $\min(x_t, x_{t-1}) = x_{t-1} - \text{ReLU}(x_{t-1} - x_t)$

Figure 4: Algorithm extraction results for `maximum_prev2` and `minimum_prev2` tasks. The top panel shows the raw code where sub-MLPs utilize ReLU functions to compare the current token  $x_t$  with the previous token  $x_{t-1}$ . The bottom panel presents the simplified expressions, verifying that the model correctly reconstructs the extrema functions using the ReLU-based algebraic identities.

interpretability-aware controllability. In scientific discovery, researchers often seek not just any solution, but a specific form of algorithm that aligns with domain knowledge (Schmidt and Lipson, 2009; Udrescu and Tegmark, 2020; Cranmer et al., 2020). We address this need by explicitly manipulating the architectural constraints and training configurations of our model to impose inductive biases, thereby steering the solution space.

We demonstrate this controllability through two intervention scenarios. First, we manipulate architectural primitives. In the `maximum_prev2` task, the unconstrained model typically solves maximization via MLP-based arithmetic approximation (exploiting ReLU non-linearity). To test if the model can switch algorithmic paradigms, we explicitly set the number of sub-MLPs to zero, removing its capacity for complex arithmetic. Consequently, the model adapts by shifting its entire mechanism to the Numerical Attention module. It discovers

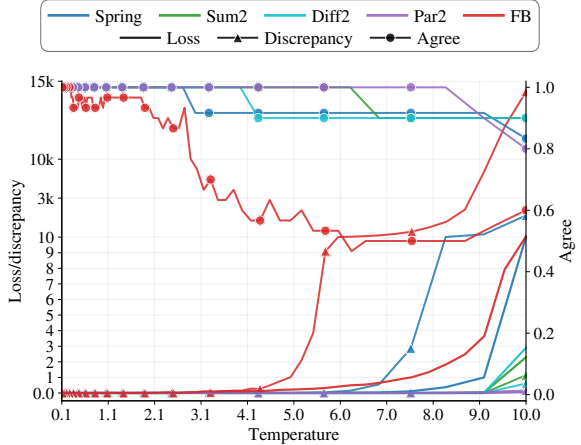


Figure 5: Training dynamics exhibit a clear phase transition: the loss decreases earlier, while the pronounced drop in Discrepancy occurs slightly later, coinciding with Agreement approaching 1.0 during temperature annealing from 10.0 to 1.0. The abbreviations Spring, Sum2, Diff2, Par2, and FB denote the `spring`, `sum_last2`, `diff_last2`, `parity_last2`, and `freebody` tasks, respectively.

a “windowed max” attention pattern, solving the task by directly copying the largest value from the context rather than computing it. Second, we intervene in the information flow. In the `spring` task, the model typically learns the standard recurrence  $y_i = y_{i-1} - y_{i-2} + x_i$ . By masking the immediate history  $(y_{i-1}, y_{i-2})$ , we guide the model to bypass the standard path and discover a mathematically equivalent high-order recurrence:  $y_i = -y_{i-3} + x_i + x_{i-1}$ . These findings highlight the Discrete Transformer as a robust tool for intervenable algorithm discovery, capable of uncovering multiple equivalent logical paths underlying the same data distribution.

## 7 Conclusions

In this work, we present the Discrete Transformer, a novel framework that enables program synthesis via algorithm extraction directly from Transformer architectures. By enforcing a disentangled numerical residual stream and employing a smooth discrete optimization curriculum, our model decouples information routing from arithmetic computation, facilitating the extraction of concise, human-readable algorithms. Overall, our experiments demonstrate that the Discrete Transformer not only achieves performance comparable to RNN-based baselines on diverse algorithmic tasks but also offers superior controllability, allowing users to im-

pose explicit inductive biases to guide the solution discovery.

## Limitations

Despite its promise, the Discrete Transformer exhibits inherent limitations stemming from its interpretability-driven design: (1) Complexity Ceiling: The dependence on symbolic regression restricts applicability to tasks decomposable into low-dimensional, sparse interactions rather than high-dimensional dense processing. (2) Restricted Expressivity: Formulating attention as a hard information router constrains model expressiveness, inherently limiting performance on tasks that necessitate the continuous, graded weighting mechanisms of soft attention. (3) Capacity Trade-off: Enforcing disentangled scalar representations sacrifices the compressive efficiency of superposition, thereby limiting the capacity required for general natural language understanding tasks that rely on distributed and entangled features.

## Impact Statement

This paper advances the fields of mechanistic interpretability and algorithm extraction by enabling the discovery of verifiable, human-readable programs from the Discrete Transformer. There are many potential societal consequences of our work, none of which we feel must be specifically highlighted here.

## References

Trenton Bricken, Adly Templeton, Joshua Batson, Brian Chen, Adam Jermyn, Tom Conerly, Nick Turner, Cem Anil, Carson Denison, Amanda Askell, Robert Lasenby, Yifan Wu, Shauna Kravec, Nicholas Schiefer, Tim Maxwell, Nicholas Joseph, Zac Hatfield-Dodds, Alex Tamkin, Karina Nguyen, and 6 others. 2023. Towards monosemanticity: Decomposing language models with dictionary learning. *Transformer Circuits Thread*. [Https://transformer-circuits.pub/2023/monosemantic-features/index.html](https://transformer-circuits.pub/2023/monosemantic-features/index.html).

Alonzo Church. 1963. Application of recursive arithmetic to the problem of circuit synthesis. *Journal of Symbolic Logic*, 28(4).

Miles Cranmer. 2023. [Interpretable machine learning for science with pysisr and symbolicregression.jl](#). *Preprint*, arXiv:2305.01582.

Miles Cranmer, Alvaro Sanchez-Gonzalez, Peter Battaglia, Rui Xu, Kyle Cranmer, David Spergel, and Shirley Ho. 2020. [Discovering symbolic models from deep learning with inductive biases](#). *Preprint*, arXiv:2006.11287.

Hoagy Cunningham, Aidan Ewart, Logan Riggs, Robert Huben, and Lee Sharkey. 2023. [Sparse autoencoders find highly interpretable features in language models](#). *Preprint*, arXiv:2309.08600.

Nelson Elhage, Tristan Hume, Catherine Olsson, Nicholas Schiefer, Tom Henighan, Shauna Kravec, Zac Hatfield-Dodds, Robert Lasenby, Dawn Drain, Carol Chen, Roger Grosse, Sam McCandlish, Jared Kaplan, Dario Amodei, Martin Wattenberg, and Christopher Olah. 2022. [Toy models of superposition](#). *Preprint*, arXiv:2209.10652.

Dan Friedman, Alexander Wettig, and Danqi Chen. 2023. Learning transformer programs. *Advances in Neural Information Processing Systems*, 36:49044–49067.

Mor Geva, Avi Caciularu, Kevin Wang, and Yoav Goldberg. 2022. [Transformer feed-forward layers build predictions by promoting concepts in the vocabulary space](#). In *Proceedings of the 2022 Conference on Empirical Methods in Natural Language Processing*, pages 30–45, Abu Dhabi, United Arab Emirates. Association for Computational Linguistics.

Yury Gorishniy, Ivan Rubachev, and Artem Babenko. 2022. On embeddings for numerical features in tabular deep learning. *Advances in Neural Information Processing Systems*, 35:24991–25004.

Alex Graves, Greg Wayne, and Ivo Danihelka. 2014. [Neural turing machines](#). *Preprint*, arXiv:1410.5401.

Daya Guo, Qihao Zhu, Dejian Yang, Zhenda Xie, Kai Dong, Wentao Zhang, Guanting Chen, Xiao Bi, Y. Wu, Y. K. Li, Fuli Luo, Yingfei Xiong, and Wenfeng Liang. 2024. [Deepseek-coder: When the large language model meets programming – the rise of code intelligence](#). *Preprint*, arXiv:2401.14196.

Eric Jang, Shixiang Gu, and Ben Poole. 2017. [Categorical reparameterization with gumbel-softmax](#). *Preprint*, arXiv:1611.01144.

Quoc-Vinh Lai-Dang, Taemin Kang, and Seungah Son. 2025. [Adaptive transformer programs: Bridging the gap between performance and interpretability in transformers](#). In *International Conference on Representation Learning*, volume 2025, pages 62785–62807.

David Lindner, János Kramár, Sebastian Farquhar, Matthew Rahtz, Tom McGrath, and Vladimir Mikulík. 2023. Tracr: Compiled transformers as a laboratory for interpretability. *Advances in Neural Information Processing Systems*, 36:37876–37899.

Ilya Loshchilov and Frank Hutter. 2019. [Decoupled weight decay regularization](#). *Preprint*, arXiv:1711.05101.

Christos Louizos, Max Welling, and Diederik P. Kingma. 2018. [Learning sparse neural networks through  \$l\_0\$  regularization](#). *Preprint*, arXiv:1712.01312.

He Ma, Arunachalam Narayanaswamy, Patrick Riley, and Li Li. 2022. Evolving symbolic density functionals. *Science Advances*, 8(36):eabq0279.

André F. T. Martins and Ramón Fernandez Astudillo. 2016. [From softmax to sparsemax: A sparse model of attention and multi-label classification](#). *Preprint*, arXiv:1602.02068.

Aaron Meurer, Christopher P. Smith, Mateusz Paprocki, Ondřej Čertík, Sergey B. Kirpichev, Matthew Rocklin, AMiT Kumar, Sergiu Ivanov, Jason K. Moore, Sartaj Singh, Thilina Rathnayake, Sean Vig, Brian E. Granger, Richard P. Muller, Francesco Bonazzi, Harsh Gupta, Shivam Vats, Fredrik Johansson, Fabian Pedregosa, and 8 others. 2017. [Sympy: symbolic computing in python](#). *PeerJ Computer Science*, 3:e103.

Eric J. Michaud, Isaac Liao, Vedang Lad, Ziming Liu, Anish Mudide, Chloe Loughridge, Zifan Carl Guo, Tara Rezaei Kheirkhah, Mateja Vukelić, and Max Tegmark. 2024. [Opening the ai black box: program synthesis via mechanistic interpretability](#). *Preprint*, arXiv:2402.05110.

Adam Paszke, Sam Gross, Francisco Massa, Adam Lerer, James Bradbury, Gregory Chanan, Trevor Killeen, Zeming Lin, Natalia Gimelshein, Luca Antiga, Alban Desmaison, Andreas Köpf, Edward Yang, Zach DeVito, Martin Raison, Alykhan Tejani, Sasank Chilamkurthy, Benoit Steiner, Lu Fang, and 2 others. 2019. [Pytorch: An imperative style, high-performance deep learning library](#). *Preprint*, arXiv:1912.01703.

Colin Raffel, Noam Shazeer, Adam Roberts, Katherine Lee, Sharan Narang, Michael Matena, Yanqi Zhou, Wei Li, and Peter J. Liu. 2023. [Exploring the limits of transfer learning with a unified text-to-text transformer](#). *Preprint*, arXiv:1910.10683.

Baptiste Rozière, Jonas Gehring, Fabian Gloclekle, Sten Sootla, Itai Gat, Xiaoqing Ellen Tan, Yossi Adi, Jingyu Liu, Romain Sauvestre, Tal Remez, Jérémie Rapin, Artyom Kozhevnikov, Ivan Evtimov, Joanna Bitton, Manish Bhatt, Cristian Canton Ferrer, Aaron Grattafiori, Wenhan Xiong, Alexandre Défossez, and 7 others. 2024. [Code llama: Open foundation models for code](#). *Preprint*, arXiv:2308.12950.

Pedro Savarese, Hugo Silva, and Michael Maire. 2021. [Winning the lottery with continuous sparsification](#). *Preprint*, arXiv:1912.04427.

Michael Schmidt and Hod Lipson. 2009. Distilling free-form natural laws from experimental data. *Science*, 324(5923):81–85.

Parshin Shojaee, Kazem Meidani, Shashank Gupta, Amir Barati Farimani, and Chandan K. Reddy. 2025. [Llm-sr: Scientific equation discovery via programming with large language models](#). *Preprint*, arXiv:2404.18400.

CodeGemma Team, Heri Zhao, Jeffrey Hui, Joshua Howland, Nam Nguyen, Siqi Zuo, Andrea Hu, Christopher A. Choquette-Choo, Jingyue Shen, Joe Kelley, Kshitij Bansal, Luke Vilnis, Mateo Wirth, Paul Michel, Peter Choy, Pratik Joshi, Ravin Kumar, Sarmad Hashmi, Shubham Agrawal, and 8 others. 2024. [Codegemma: Open code models based on gemma](#). *Preprint*, arXiv:2406.11409.

Silviu-Marian Udrescu, Andrew Tan, Jiahai Feng, Orisvaldo Neto, Tailin Wu, and Max Tegmark. 2020. [Ai feynman 2.0: Pareto-optimal symbolic regression exploiting graph modularity](#). *Preprint*, arXiv:2006.10782.

Silviu-Marian Udrescu and Max Tegmark. 2020. [AI Feynman: A physics-inspired method for symbolic regression](#). *Science Advances*, 6(16):eaay2631.

Gail Weiss, Yoav Goldberg, and Eran Yahav. 2021. [Thinking like transformers](#). *Preprint*, arXiv:2106.06981.

Yifan Zhang, Wenyu Du, Dongming Jin, Jie Fu, and Zhi Jin. 2025. [Finite state automata inside transformers with chain-of-thought: A mechanistic study on state tracking](#). *Preprint*, arXiv:2502.20129.

## A Smooth Transition Mechanism for Discrete Optimization

To train the discrete selection parameters in our discretized reading and Numerical Attention modules, we address the non-differentiability of hard selection while avoiding the pitfalls of standard relaxation methods. While Gumbel-Softmax enables differentiable sampling, it often struggles to escape local optima and fails to promote the strict sparsity essential for interpretability. To address this, we incorporate a smooth transition mechanism (Lai-Dang et al., 2025), which dynamically interpolates between Gumbel-Softmax and Sparsemax (Martins and Astudillo, 2016) throughout the training process. The hybrid sampling vector  $\mathbf{p} \in \mathbb{R}^{N_t}$  is defined as:

$$\mathbf{p} = (1 - \alpha(\tau))\mathbf{p}_{\text{soft}} + \alpha(\tau)\mathbf{p}_{\text{sparse}}, \quad (8)$$

where  $\mathbf{p}_{\text{soft}}$  and  $\mathbf{p}_{\text{sparse}}$  denote sample vectors drawn from Gumbel-Softmax and Gumbel-Sparsemax distributions, respectively. The interpolation coefficient  $\alpha(\tau) \in [0, 1]$  is a scheduler function of the temperature  $\tau$ , designed to shift strictly from 0 to 1 as  $\tau$  anneals. This mechanism allows the model to prioritize exploration via Softmax in the early stages, before smoothly transitioning to

Sparsemax to enforce sparsity and deterministic selection (exploitation) in later stages. Ultimately, this ensures convergence to concise, interpretable program structures.

## B Unmatched Heads

While the *Fixed Offset* and *Windowed Extrema* patterns achieve high coverage across the algorithmic benchmark investigated, we observe a subset of attention heads that do not conform to these interpretability templates. Crucially, our analysis reveals that these “unmatched heads” do not represent missing algorithmic primitives, but rather manifest as computational noise or redundancy. We observe that these heads are generally rendered ineffective through two primary mechanisms: by being suppressed with negligible magnitudes, or by being ignored by higher-layer modules.

For instance, in the `bitwise_and` task, the head labeled `Attn_L0H1` exhibits a disordered attention matrix that matches neither location-based nor content-based patterns. However, symbolic tracing of the computational graph confirms that its output variable is an orphan variable: it is not selected as an input by any subsequent modules nor aggregated by the final output projection. Similarly, in the `minimum_prev2` task with the number of sub-MLPs constrained to zero, we observe that the head labeled `Attn_L0H1` behaves as an unmatched head. Since its output is disconnected from the valid execution path, this lack of interpretability does not impede successful extraction of the underlying algorithm.

## C Experiment Details

**Datasets** We adopt the algorithmic reasoning suite from the MIPS benchmark (Michaud et al., 2024) as our primary testbed. These tasks probe specific capabilities of neural networks, such as arithmetic reasoning, variable tracking, and non-linear composition. We categorize them into three logical tiers based on their underlying complexity and memory dependence:

- **Linear Arithmetic (Local vs. Global).** This category involves linear transformations. *Non-state-tracking* tasks (e.g., `sum_last2`) require only local attention within a fixed window. In contrast, *State-tracking* tasks (e.g., `sum_last`) require the model to maintain a persistent memory state—implicitly simulating a finite state automaton (Zhang et al., 2025)—to compute cumulative metrics over the

sequence.

- **Non-Linear Composition.** These tasks necessitate non-linear activation logic. Variants range from local operations like `parity_last2` and `maximum_prev2` to global state-tracking tasks like `add_mod_3`. Success here requires the Numerical MLP to approximate non-linear functions (e.g., XOR) rather than simple linear aggregation.

- **Dynamical Systems (Physical Problems).** To evaluate generalization beyond pure arithmetic, we include tasks derived from classical mechanics (`freebody`, `gravity`, and `spring`). While mathematically reducible to iterative linear updates, these tasks challenge the model to discover governing physical laws (e.g., Newton’s laws of motion) and simulate continuous dynamical systems purely from observed data.

**Training Details** All models adopt a decoder-only architecture implemented in PyTorch (Paszke et al., 2019), optimized via AdamW (Loshchilov and Hutter, 2019) to minimize MSE. The training dataset consists of 1,000,000 samples. Unless otherwise specified, both the input and output sequences have a fixed length of 10. We employ a cosine annealing schedule to decay the learning rate from 0.05 to  $1 \times 10^{-6}$  over 50 epochs with a batch size of 512. (For the `freebody` and `gravity` tasks, models are trained for 100 epochs with an initial learning rate of 0.01.) To handle discrete optimization, we apply a geometric annealing schedule to the sampling temperature  $\tau$ , decreasing it from 10.0 to 0.1 to facilitate a gradual transition from continuous exploration to discrete selection. For each task, we conduct a grid search over the number of layers {1, 2}, attention heads {2, 3}, and sub-MLPs per layer {2, 3}. We run all experiments across three random seeds, reporting the mean performance and selecting the checkpoint with the best validation performance for subsequent analysis.

**Task Formulation** To facilitate algorithm extraction and ensure robustness across varying sequence lengths and positions, we design our task formulations to encourage the learning of length-invariant functions. We categorize tasks based on their reliance on state-tracking: (1) Non-state-tracking tasks are formulated as Token-Tagging problems, requiring independent, element-wise predictions for each position. (2) State-tracking tasks are framed as Language Modeling problems, where the model performs autoregressive next-token prediction based on the input and historical context. To facilitate symbolic regression and align with

the regression nature of the task, we adopt MSE as the loss function, enabling the model to learn continuous functional mappings.

## D Sensitivity Analysis of Model Capacity

To evaluate the robustness of our framework under architectural variations, we investigate the impact of hyperparameters—specifically the number of layers, attention heads per layer, and sub-MLPs per layer—on both the convergence quality, measured by the MSE loss, and the interpretability, quantified by the line count of the extracted program. We conduct experiments on the `sum_last2`, `parity_last2`, and `spring` tasks, varying the number of layers in  $\{1, 2, 3, 4\}$ , attention heads per layer in  $\{0, 1, 2, 4, 8\}$ , and sub-MLPs per layer in  $\{0, 1, 2, 4, 8\}$ .

Our results exhibit a clear threshold effect in expressive capacity. Once the architecture satisfies the minimal functional requirements of the target task (e.g., `sum_last2` requires at least one attention head to retrieve the token  $x_{t-1}$ ), the Discrete Transformer reliably converges to a near-zero MSE loss. In contrast, over-parameterization substantially alters the dynamics of the discrete search. Specifically, excessive capacity tends to inflate the length of the extracted programs due to structural redundancy: multiple modules may learn functionally equivalent behaviors (e.g., several attention heads learning the same retrieval pattern for  $x_{t-1}$ ). The introduction of redundant modules expands the search space and introduces noise during the exploration phase. While this poses a challenge to the optimization stability, we find that it can be effectively addressed by adopting a slower temperature annealing schedule, which provides sufficient time to resolve the competition between redundant components and settle into a valid discrete solution.

## E Additional Synthesized Programs

This section, we provide additional synthesized programs.

```

1 import numpy as np
2 def maximum_prev2(input_seq):
3     # V0_input
4     input_arr = np.array(input_seq, dtype=float)
5     seq_len = input_arr.shape[0]
6     V0 = input_arr[:, 0]
7     # V1_Attn_L0H0
8     V1 = np.zeros(seq_len)
9     # windowed max
10    for t in range(seq_len):
11        V1[t] = np.max(V0[max(0, t-1): t+1])
12    # V2_Attn_L0H1
13    V2 = np.zeros(seq_len)
14    # windowed max
15    for t in range(seq_len):
16        V2[t] = np.max(V0[max(0, t-1): t+1])
17    # Output Head
18    output = 1.07 * V1 + -0.07 * V2
19    return output
20

```

```

1 import numpy as np
2 def minimum_prev2(input_seq):
3     # V0_input
4     input_arr = np.array(input_seq, dtype=float)
5     seq_len = input_arr.shape[0]
6     V0 = input_arr[:, 0]
7     # V1_Attn_L0H0
8     V1 = np.zeros(seq_len)
9     # windowed min
10    for t in range(seq_len):
11        V1[t] = np.min(V0[max(0, t-1): t+1])
12    # Output Head
13    output = 1.00 * V1
14    return output
15

```

```

1 import numpy as np
2 def spring(input_seq):
3     # V0_input
4     input_arr = np.array(input_seq, dtype=float)
5     seq_len = input_arr.shape[0]
6     V0 = input_arr[:, 0]
7     # V1_Attn_L0H0
8     V1 = np.zeros(seq_len)
9     # Fixed offset 9
10    V1[9:] = V0[:-9]
11    # V2_Attn_L0H1
12    V2 = np.zeros(seq_len)
13    # Fixed offset 10
14    V2[10:] = V0[:-10]
15    # V3_MLP_L0M0
16    V3 = np.full(seq_len, 0.02)
17    # V4_MLP_L0M1
18    V4 = np.full(seq_len, -0.11)
19    # V5_Attn_L1H0
20    V5 = np.zeros(seq_len)
21    # Fixed offset 2
22    V5[2:] = V0[:-2]
23    # V6_Attn_L1H1
24    V6 = np.zeros(seq_len)
25    # Fixed offset 2
26    V6[2:] = V4[:-2]
27    # V7_MLP_L1M0
28    V7 = np.full(seq_len, -0.03)
29    # Output Head
30    output = 1.00 * V1 + 1.00 * V2 + -1.00 * V5 + 0.03 *
31        V7 + -0.01 * V6
32    return output

```

Figure 6: Intervened synthesized programs revealing alternative logical pathways. Left: When MLP-based arithmetic is prohibited, the model solves `maximum_prev2` and `minimum_prev2` by shifting to a pure attention mechanism. The extracted code shows explicit *Windowed Extrema* attention patterns. Right: For the `spring` task, intervention in the information flow (masking recent history) forces the model to learn a high-order recurrence relation, validating the model’s ability to uncover multiple equivalent algorithms for the same data distribution.

```

1 import numpy as np
2 def sum_last(input_seq):
3     # V0_input
4     input_arr = np.array(input_seq, dtype=float)
5     seq_len = input_arr.shape[0]
6     V0 = input_arr[:, 0]
7     # V1_Attn_L0H0
8     V1 = np.zeros(seq_len)
9     # Fixed offset 9
10    V1[9:] = V0[:-9]
11    # Output Head
12    output = 1.00 * V0 + 1.00 * V1
13    return output
14

```

```

1 import numpy as np
2 def bitwise_and(input_seq):
3     # V0_input, V1_input
4     input_arr = np.array(input_seq, dtype=float)
5     seq_len = input_arr.shape[0]
6     V0_input = input_arr[:, 0]
7     V1_input = input_arr[:, 1]
8     # V4_MLP_L0M0
9     V4 = np.full(seq_len, 0.02)
10    # V5_MLP_L0M1
11    V5 = (((V0 - 0.49) * 3.28) / (V1 + -0.52)) - 3.06 *
12        0.19
13    # Output Head
14    output = 0.49 * V1 + 0.48 * V0 + 0.40 * V5 + 0.02 *
15        V4
16    return output
17

```

```

1 import numpy as np
2 def add_mod_3(input_seq):
3     # V0_input
4     input_arr = np.array(input_seq, dtype=float)
5     seq_len = input_arr.shape[0]
6     V0 = input_arr[:, 0]
7     # V1_Attn_L0H0
8     V1 = np.zeros(seq_len)
9     # Fixed offset 9
10    V1[9:] = V0[:-9]
11    # V2_Attn_L0H1
12    V2 = np.zeros(seq_len)
13    # Fixed offset 9
14    V2[9:] = V0[:-9]
15    # V3_MLP_L0M0
16    V3 = ((-0.70 / (((V0 + V1) + 0.59) * -0.56)) - 1.69) +
17        (1.05 / (V0 + (V1 - 2.53)))
18    # Output Head
19    output = -0.53 * V3 + 0.47 * V2 + -0.32 * V1 + 0.16 *
20        V0
21    return output
22

```

Figure 7: Synthesized programs for sum\_last (Top Left), bitwise\_and (Bottom Left), and add\_mod\_3 (Right).

Table 2: Performance and parameters of the Discrete Transformer on the algorithmic benchmark. The columns Layers, Heads, and sub-MLPs correspond to the number of layers, the number of attention heads per layer, and the number of sub-MLPs per layer, respectively. Loss values indicate MSE for these regression tasks.

Task Name	Description	Layers	Heads	sub-MLPs	Train Loss	Test Loss
<i>Linear Arithmetic</i>						
sum_last2	Sum of the last two numbers	1	2	2	$8.82 \times 10^{-9}$	$6.76 \times 10^{-9}$
diff_last2	Difference between last two numbers	1	2	2	$6.59 \times 10^{-16}$	$7.02 \times 10^{-16}$
sum	Cumulative sum of the sequence	1	2	2	$1.71 \times 10^{-14}$	$1.70 \times 10^{-14}$
<i>Non-Linear Composition</i>						
parity_last2	Parity check of the last two numbers	1	2	2	$4.87 \times 10^{-13}$	$1.46 \times 10^{-12}$
maximum_prev2	Maximum of the last two numbers	1	2	2	$1.11 \times 10^{-6}$	$4.43 \times 10^{-6}$
minimum_prev2	Minimum of the last two numbers	1	2	2	$1.64 \times 10^{-5}$	$1.77 \times 10^{-5}$
bitwise_and	Bitwise AND	1	2	2	$1.10 \times 10^{-18}$	$1.06 \times 10^{-18}$
bitwise_or	Bitwise OR	1	2	2	$5.66 \times 10^{-4}$	$1.63 \times 10^{-6}$
bitwise_not	Bitwise NOT	1	2	2	$1.44 \times 10^{-17}$	$< 10^{-20}$
bitwise_xor	Bitwise XOR	1	2	2	$6.74 \times 10^{-20}$	$6.67 \times 10^{-20}$
abs	Absolute value of the current number	1	2	2	$2.69 \times 10^{-14}$	$5.25 \times 10^{-14}$
abs_of_diff	Absolute difference of last two numbers	1	2	2	$9.72 \times 10^{-9}$	$2.01 \times 10^{-8}$
parity	Cumulative parity	1	2	2	$8.15 \times 10^{-17}$	$8.09 \times 10^{-17}$
add_mod_3	Cumulative sum modulo 3	1	2	2	$9.72 \times 10^{-13}$	$1.72 \times 10^{-7}$
<i>Physical Problems</i>						
freebody	Simulate freebody dynamics	2	2	3	$9.57 \times 10^{-11}$	$9.57 \times 10^{-11}$
gravity	Simulate gravity dynamics	2	2	3	$2.34 \times 10^{-11}$	$1.86 \times 10^{-11}$
spring	Simulate spring dynamics	1	2	2	$1.41 \times 10^{-7}$	$3.49 \times 10^{-9}$

```

1 import numpy as np
2 def freebody(input_seq):
3     # V0_input
4     input_arr = np.array(input_seq, dtype=float)
5     seq_len = input_arr.shape[0]
6     V0 = input_arr[:, 0]
7     # V1_Attn_L0H0
8     V1 = np.zeros(seq_len)
9     # Fixed offset 9
10    V1[9:] = V0[:-9]
11    # V2_Attn_L0H1
12    V2 = np.zeros(seq_len)
13    # Fixed offset 10
14    V2[10:] = V0[:-10]
15    # V4_MLP_L0M1
16    V4 = -0.26*V0 + 0.04
17    # V5_MLP_L0M2
18    V5 = -0.21*V0 + -0.04
19    # V6_Attn_L1H0
20    V6 = np.zeros(seq_len)
21    # Fixed offset 2
22    V6[2:] = V4[:-2]
23    # V7_Attn_L1H1
24    V7 = np.zeros(seq_len)
25    # Fixed offset 2
26    V7[2:] = V5[:-2]
27    # Output Head
28    output = 1.19 * V0 + 1.06 * V7 + 1.06 * V6 + 1.00 *
29    V1 + -0.65 * V4 + -0.65 * V5 + 0.50 * V2
30    return output

```

```

1 import numpy as np
2 def gravity(input_seq):
3     # V0_input
4     input_arr = np.array(input_seq, dtype=float)
5     seq_len = input_arr.shape[0]
6     V0 = input_arr[:, 0]
7     # V1_Attn_L0H0
8     V1 = np.zeros(seq_len)
9     # Fixed offset 9
10    V1[9:] = V0[:-9]
11    # V2_Attn_L0H1
12    V2 = np.zeros(seq_len)
13    # Fixed offset 10
14    V2[10:] = V0[:-10]
15    # V4_MLP_L0M1
16    V4 = 0.00
17    # V5_MLP_L0M2
18    V5 = -0.40*V0 + -3.05
19    # V6_Attn_L1H0
20    V6 = np.zeros(seq_len)
21    # Fixed offset 2
22    V6[2:] = V5[:-2]
23    # V7_Attn_L1H1
24    V7 = np.zeros(seq_len)
25    # Fixed offset 2
26    V7[2:] = V4[:-2]
27    # Output Head
28    output = 1.24 * V6 + 1.20 * V0 + 1.00 * V1 + -0.74 *
29    V5 + 0.50 * V2 + -0.01 * V4 + 0.01 * V7
30    return output

```

```

1 import numpy as np
2 def spring(input_seq):
3     # V0_input
4     input_arr = np.array(input_seq, dtype=float)
5     seq_len = input_arr.shape[0]
6     V0 = input_arr[:, 0]
7     # V1_Attn_L0H0
8     V1 = np.zeros(seq_len)
9     # Fixed offset 9
10    V1[9:] = V0[:-9]
11    # V2_Attn_L0H1
12    V2 = np.zeros(seq_len)
13    # Fixed offset 1
14    V2[1:] = V0[:-1]
15    # V4_MLP_L0M1
16    V4 = (V2 + ((V1 - ((V1 + 2.26) + (V2 - 1.54))) * 2.00)
17    ) + (V2 + 1.43)
18    # Output Head
19    output = -1.00 * V2 + 1.00 * V0 + 1.00 * V1 + 0.04 *
20    V4
21    return output

```

Figure 8: Synthesized programs for `freebody` (Top Left), `spring` (Bottom Left), and `gravity` (Right). By coordinating Numerical Attention, Numerical MLP and the output head, the model effectively identifies essential computational variables and constructs the correct computation graph. This confirms the model’s capability to learn underlying physical laws and demonstrates its potential for modeling complex physical processes.